Study of the electronic structure of transition metal compounds by absorption and emission of X-rays

J. Jiménez-Mier[a], G. Herrera-Pérez[a,b], P. Olalde-Velasco[a], E. Chavira[b], I. Jiménez-DelVal[c], and D.L. Ederer[d]
[a]*Instituto de Ciencias Nucleares, Universidad Nacional Autónoma de México, 04510 México D.F., México.*
[b]*Instituto de Investigaciones en Materiales, Universidad Nacional Autónoma de México, 04510 México D.F., México.*
[c]*Facultad de Quımica, Universidad Nacional Autónoma de México, 04510, México D.F., México.*
[d]*Department of Physics, Tulane University, New Orleans, Louisiana 70118, U.S.A.*

Recibido el 2 de marzo de 2006; aceptado el 18 de agosto de 2006

We present results of x-ray absorption and x-ray emission spectroscopies of transition metal oxides and fluorides. The absorption is studied in the vicinity of the transition metal L edge. At selected values of the excitation energy we also show emission spectra. The data are interpreted in terms of the multiplet structure of the transition metal ion in a crystal field, considering also configuration interaction effects in the solid such as charge transfer. The data are compared with results of free-ion calculations that allow a direct interpretation of the absorption spectra. The free-ion calculations also indicate that some of the main emission features correspond to d to d excitations in the compound, with the emission peaks with higher energy losses resulting from production of charge transfer states.

Keywords: Synchrotron radiation; x-ray absorption and emission; transition metal oxides and fluorides; electronic structure.

Se presentan resultados de espectroscopias de absorción y emisión de rayos x de óxidos y fluoruros de metales de transición. Se estudia la absorción en la cercanía de la orilla L de absorción del metal de transición. Para algunos valores de la enegía de excitación también se muestran espectros de emisión. Los datos se interpretan en términos de la estructura de multiplete del ion del metal de transición en un campo cristalino, considerando también efectos de interacción de configuraciones en el sólido, como es la transferencia de carga. Se comparan los datos con resultados de un cálculo para ion libre que permite una interpretación directa de los espectros de absorción. Los cálculos para iones libres también indican que algunos de los picos de emisión más importantes corresponden a la producción de excitadiones d a d en el compuesto, con picos de emisión a más altas energías de pérdida debidos a estados de transferencia de carga.

Descriptores: Radiación de sincrotrón; absorción y emisión de rayos x; óxidos y fluoruros de metales de transición; estructura electrónica.

PACS: 78.70.Ck; 78.70.En

X-ray spectroscopies have become very useful tools to study the electronic structure of complex compounds. The ability to tune the photon energy, together with the high resolution and flux atainable at synchrotron radiation sources has made possible experiments that provide very detailed information about the electronic structure of such compounds [1]. This is particularly useful for $3d$ transition metal compounds that are inherently complex due to the presence of partially filled d-subshell. X-ray absorption spectroscopy in the region of the transition metal L edge gives information about unoccupied states in the compound. Because it is an electric dipole transition, the absorption process selects unoccupied states of d character, which are precisely the ones responsible for the complex behavior of the system. Normal X-ray emission follows the non-resonant production of a core $2p$ hole and its subsequent radiative decay provides information about the occupied d states in the transition metal in a higher ionization state. X-ray emission that follows the *resonant* $2p \rightarrow 3d$ excitation at the L absorption edge [1] allows the study of the electronic structure of the transition metal in its original ionic state .

In this work we present x-ray absorption spectra recorded at the transition metal L-edge of TiF_4, TiO_2, MnF_2, MnO, and CoF_2. The results are compared with single-configuration Hartree-Fock free-ion calculations that allow a direct interpretation of the states populated in the absorption and then in the decay process. We also show resonant x-ray emission spectra for each compound. These emission spectra are interpreted in terms of the d to d excitation energies in the transition metal, including the possibility of charge transfer from the ligand.

The experiments took place at beam line 8.0.1 of The Advanced Light Source in Berkeley. Details of the beam line can be found elsewhere [2]. The radiation is produced in a 5.0 period undulator. It is monochromatized by one of three gold coated spherical gratings and then it is focused onto the sample. The x-ray absorption signal is monitored by the total sample current. This results in total electron yield (TEY) spectra. The monochromator photon energy was calibrated with TiO_2 and metallic copper TEY spectra. This covers the entire energy region between 440 and 960 eV, and we estimate it to be accurate within 0.4 eV. At selected values of the excitation energy of each TEY spectra we also record x-ray emission spectra. This is done at a low-background soft x-ray spectrometer [2]. It detects photons emitted at right angles with respect to the incoming beam, along its polarization

direction. It has four different gratings that cover the photon energy range between 100 and at least 1000 eV. A variable entrance slit allows control over the spectrometer resolution. The emission spectra are recorded with a position sensitive detector mounted along the Rowland circle. In all samples studied there was resonant elastic emission that allowed the calibration of the spectrometer photon energy. The fluorides and the MnO were all commercial powders of purity greater than 98%. The TiO_2 was a polycrystalline sample that was compressed into a pellet that was later annealed to 1100° during four days. Powder x-ray diffraction studies indicate that this sample was TiO_2 in the rutile phase. All emission spectra presented in this work are corrected for self absorption [3, 4].

Resonant x-ray absorption and emission is a coherent second order process that is described by the Kramers-Heisenberg expression:

$$\sigma(\nu_1,\nu_2) \propto \sum_f |\sum_i \frac{\langle f|\vec{e}_2\cdot\vec{r}|i\rangle\langle i|\vec{e}_1\cdot\vec{r}|g\rangle}{h\nu_1-(E_i-E_g)-i\Gamma_i/2}|^2 \times \delta[h(\nu_1-\nu_2)-(E_f-E_g)] \quad (1)$$

where $|g\rangle$, $|i\rangle$ and $|f\rangle$ are the initial-, intermediate-, and final-state wavefunctions with energies E_g, E_i, and E_f respectively. The transition operator $\vec{e}\cdot\vec{r}$ assumes that all are electric dipole transitions, and the delta function assures overall conservation of energy. In this paper we make the simplest assumptions to evaluate this expression [4]. We calculate the wavefunctions and the transition matrix elements using free-ion single-configuration Hartree-Fock calculations [5]. For the transition metal ions these calculations start with a $3d^n$ ground configuration ($n = 0$ for Ti^{4+}, 5 for Mn^{2+}, and 7 for Co^{2+}). One then calculates the states that result from an electric dipole excitation of a $2p$ electron into the $2p^5\ 3d^{n+1}$ configuration. In the present calculation we also neglect the interference terms in Eq. (1). We also evaluate it at resonance, which makes the Lorentzian denominator equal to the $2p$ core width squared.

In this free-ion no-interference approximation an absorption spectrum is obtained by considering all transitions that start in the lowest energy states of the ground configuration that have significant population at room temperature. Each transition energy is equal to the difference in energy between the ground and excited states, and its intensity is proportional to the square of the electric dipole transition matrix element [5]. For each absorption transition we obtain an emission spectrum by considering all electric dipole transitions from the excited state into states in the $3d^n$ ground configuration [4]. The intensity of each emission line is then proportional to the product of squares of transition matrix elements $|\langle f|\vec{e}_2\cdot\vec{r}|i\rangle|^2|\langle i|\vec{e}_1\cdot\vec{r}|g\rangle|^2$

The ground state in Ti^{4+} is simply a $3d^0\ ^1S$ term. Under strict LS coupling the only state that can be excited in the $2p^5\ 3d^1$ configuration is the ^1P. However, the spin-orbit interaction of the $2p$ hole strongly mixes LS terms and one can excite three states that have a value of the total angular momentum $J = 1$ [6]. The ligand field also plays a significant role, resulting in the splitting of the d^1 configuration into the t_{2g} and e_g levels [6]. In a simple free-ion calculation decay will only proceed to the ^1S ground state, and one only expects elastic emission (that is, the photon energy of the outgoing electron is the same as the photon energy of the incoming electron). However, a more elaborate model includes the possibility of charge transfer from the ligands [3]. In this case the ground state does not result from only the $3d^0$ configuration, but there is some mixing with a $3d^1\ \underline{\mathrm{L}}$ configuration, where $\underline{\mathrm{L}}$ represents a ligand hole. Inelastic emission is then possible by decay into excited states of this configuration admixture. In this work no attempt is made to explicitly include in the calculation any charge transfer effects.

For Mn^{2+} the ground state of the $3d^5$ configuration is the high spin ^6S term. Excitation of a $2p$ electron then results into a group of states that have the term $2p^5\ 3d^6\ ^6P$ mixed in Refs. 4 and 7. These excited states are heavily mixed spin states and therefore decay will proceed into the ^6S ground state by elastic emission and also into lower spin states (quartets and doublets) of the ground configuration [4, 8]. Therefore the emission spectra contain information about the energy necessary to flip a spin in the $3d^5$ configuration. In the manganese compounds one also expects charge transfer effects similar to the ones discussed for titanium. Once again, the theoretical results presented here do not explicitly include charge transfer effects.

The ground configuration $3d^7$ in Co^{2+} gives raise to a ^4F ground term that is split by the $3d$ spin-orbit interaction into four states with different values of the total angular momentum J. Only one of these states, namely the $J = 9/2$ has non-negligible population at room temperature and thus x-ray absorption in Co^{2+} starts also in a single high-spin and also high J state. X-ray absorption occurs into states in the $2p^5\ 3d^8$ configuration that can be produced by an electric dipole transition from this $^4F_{9/2}$ state. As in the case of Mn^{2+} [4] the states in the $Co\ (3d^7)$ ground configuration are in general well described in LS-coupling. The excited states in the $2p^5\ 3d^7$ configuration are heavily mixed, and neither LS-coupling nor jj-coupling are adequate. Decay into lower spin states (in this case doublets) or into lower ^4P term are therefore possible.

A comparison between the calculated absorption spectra of Mn^{2+} and Co^{2+} and the measured spectra of MnF_2 and CoF_2 is made in Fig. 1. The theoretical spectra are shown at the top panels, and the experimental spectra are shown at the bottom. The theoretical results are given as vertical lines whose heights are proportional to the transition intensity, and also by a continuous line that is the result of adding equal-width Gaussians centered at each line. Here it is important to point out that the overall energy scale of the calculation is shifted to match the experimental spectra. In both cases there is good agreement between experiment and theory, indicating that the main effects are already included in the free-ion model. In Mn^{2+} theory predicts a strong peak at about $640\ eV$ followed by three peaks of decreasing intensity, all

due to excitation producing a $2p_{3/2}$ hole. At about $650\ eV$ there are two peaks that result from production of a $2p_{1/2}$ hole. The TEY spectrum of MnF_2 shows the same features. However, there is also a shoulder on the low energy side of the main peak at $640\ eV$, and the first of the $2p_{1/2}$ peaks at 649 eV is also split in the experimental spectrum. These are effects due to the ligand field, and once they are included the agreement between theory and experiment is even better [4]. A similar situation occurs for Co^{2+}. Theory predicts a dominant group of three peaks at 778 eV, with shoulders at both its low and high energy sides. These all correspond to production of a $2p_{3/2}$ hole. Then there are two peaks above $790\ eV$ that result from production of a $2p_{1/2}$ hole. The experiment shows a similar structure, but with different energy splittings and peak intensities. Here again the main discrepancies are due to the ligand field. The broadening of the strong $2p_{1/2}$ peak at 792 eV is partly due to the crystal field, but there is also an effect due to a Coster-Kronig transition that transfers the $2p_{1/2}$ hole into a $2p_{3/2}$ hole with emission of a valence electron into the continuum. This decay reduces the lifetime of the $2p_{1/2}$ hole and therefore increases its linewidth.

Now we make a comparison of x-ray absorption and emission between oxides and fluorides of titanium and manganese. Titanium is nominally Ti^{4+} in both TiO_2 and TiF_4, and manganese appears as Mn^{2+} in MnO and MnF_2. Differences in the x-ray spectra of these compounds should indicate differences in their electronic structure due to the chemical environment.

In Fig. 2 we make a comparison between TiO_2 and TiF_4. The TEY spectra are shown on top, and two emission spectra for each compound are given below. The TEY spectrum of TiO_2 shown to the left is the one characteristic of Ti^{4+} in a slightly distorted octahedral environment [6]. The main $2p_{3/2}$ and $2p_{1/2}$ absorption peaks are split by the ligand field into two peaks each, corresponding to excitation into the t_{2g} (indicated by a and d) and e_g (b, c and e) levels [3]. The splitting between peaks b and c is due to the distortion from octahedral symmetry. At the high energy side of this TEY spectrum there are two weak, broad peaks that occur because of transitions into excited charge transfer states [9]. When the excitation energy is at (a) one gets the emission spectrum shown at the bottom left of Fig. 2. This spectrum has a sharp elastic peak at 458 eV with a shoulder at about 457 eV. Then there is a broad peak that is due to a valence electron filling the $2p_{3/2}$ hole centered at 450 eV. The simple free-ion model would only predict the elastic peak, and therefore this shoulder can only be due to charge transfer in the ground state of the Ti ion. The spectrum in the middle of the left side was obtained when the excitation energy is at (e). At this energy one has emission that follows the resonant production of a $2p_{1/2}$ hole and emission filling a $2p_{3/2}$ hole produced non-resonantly. Here we have the much weaker elastic peak and its shoulder at $466\ eV$ with the corresponding shoulder at 465 eV. Then there is a strong emission peak at 458 eV with a high energy shoulder just above $460\ eV$. Finally, there is the normal valence emission centered at 450 eV [3]. A more detailed analysis of the resonant x-ray emission in TiO_2 can be found in references [10] and [3].

The TEY spectrum of TiF_4 shown in Fig. 2 is significantly different. It has the main $2p_{3/2}$ and $2p_{1/2}$ peaks split by the ligand field. The splitting due to distortion from an octahedral field is different, however. There is a shoulder to the low energy side, and two more shoulders, one between a and b and the other between c and d. Then there are the two

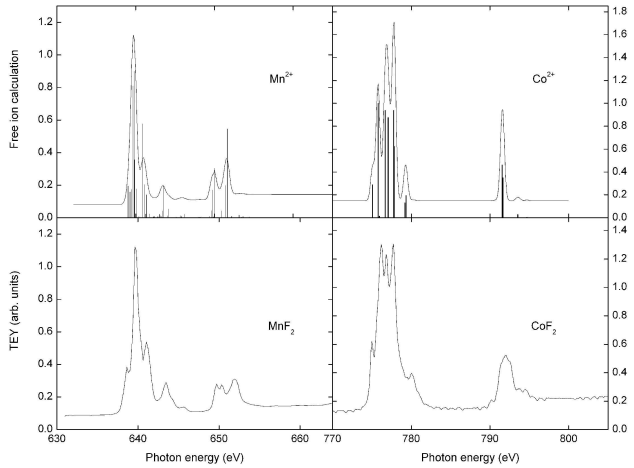

FIGURE 1. Comparison between the theoretical absorption spectra of Mn^{2+} and Co^{2+} obtained in the free-ion approximation and the experimental total electron yield spectra of MnF_2 and CoF_2. Top panels: theoretical results. The vertical lines give the predicted positions and intensities of the absorption lines. The continuous line is the result of considering the superposition of equal width Gaussians centered at each of these absorption lines. Bottom panel: TEY spectra of MnF_2 and CoF_2.

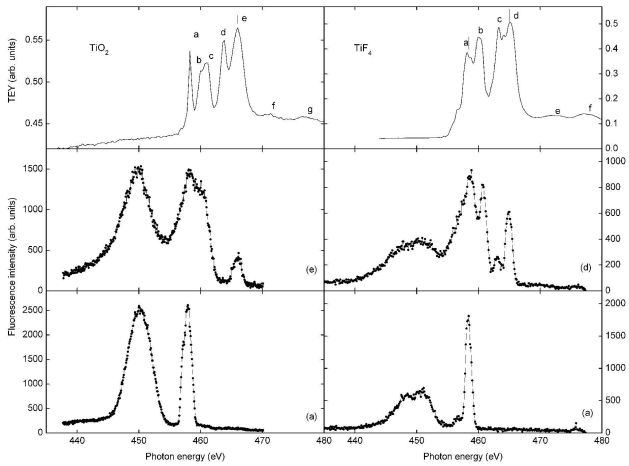

FIGURE 2. Total electron yield (TEY) and resonant emission spectra of TiO_2 (left) and TiF_4 (right). Top panel: TEY spectra. The labels indicate the resonances discussed in the text. Bottom panel: emission spectra obtained when the excitation energy is (a) in both TEY spectra. Middle panel: emission spectra obtained for excitation energies (e) in TiO_2 and (d) in TiF_4. The solid lines in the emission spectra join the experimental dots and were added to guide the eye.

charge transfer features at the high energy end of the spectrum (e and f). The emission spectrum excited at (a) is shown at the bottom of the figure. This is dominated by a strong elastic peak just above 458 eV with a smaller low energy shoulder. The separation between the elastic and this shoulder is 1.5 eV, larger than the $1.0\ eV$ found for TiO_2. The broad valence emission appears to be split into two peaks at 448 and $451\ eV$. The emission recorded when the excitation is at (d) is shown in the middle spectrum. The elastic peak at $465\ eV$ is stronger compared to TiO_2 and there is the charge transfer peak $2.0\ eV$ to its low energy side. There is a broad peak at $459\ eV$ and there is a strong narrow peak at 460.5 eV. Finally, the normal valence emission into the $2p_{3/2}$ hole is weaker than in TiO_2.

The corresponding comparison for MnO (left panel) and MnF_2 (right panel) is made in Fig. 3. The TEY spectrum of MnF_2 is the same that is shown in Fig. 1. This is the best example of a Mn^{2+} compounds. The TEY spectrum of TiO_2 shows broader features. It has been demonstrated [11,12] that this spectrum is the superposition of Mn^{2+} and Mn^{3+} absorption spectra, and that the later is due to oxidation of the powder surface. The x-ray emission spectra are less sensitive to the surface, and are thus more indicative of the sample bulk. The emission spectra are given in the lower two panels. We also show the results of multi-peak fits to each spectrum. The spectra excited at (a) in both compounds are given at the bottom of Fig. 3. They have similar structure. They both have a strong elastic peak at 640 eV. Then there are two inelastic peaks 3.1 and 5.0 eV below that result from decay into excited states of the $3d^5$ ground configuration. The ground state of this configuration is the one with maximum spin $S = 5/2$, therefore these excited states must have at least one spin of the $3d$ subshell flipped. A free ion calculation confirms

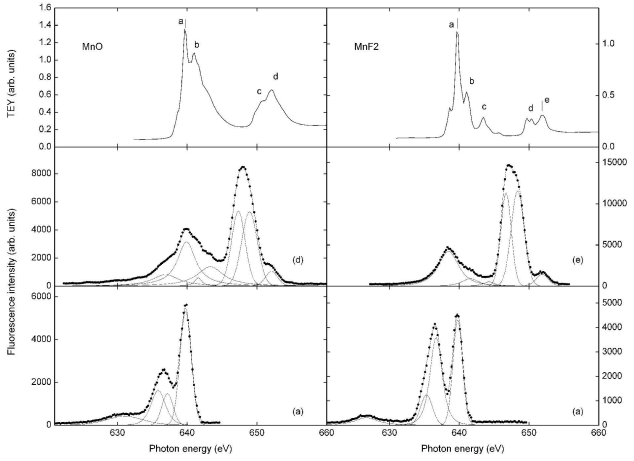

FIGURE 3. Total electron yield (TEY) and resonant emission spectra of MnO (left) and MnF_2 (right). Top panel: TEY spectra. The labels indicate the resonances discussed in the text. Bottom panel: emission spectra obtained when the excitation energy is (a) in both TEY spectra. Middle panel: emission spectra obtained for excitation energies (d) in MnO and (de) in MnF_2. The solid lines in the emission spectra are the result of multi-peak fits to the experimental data.

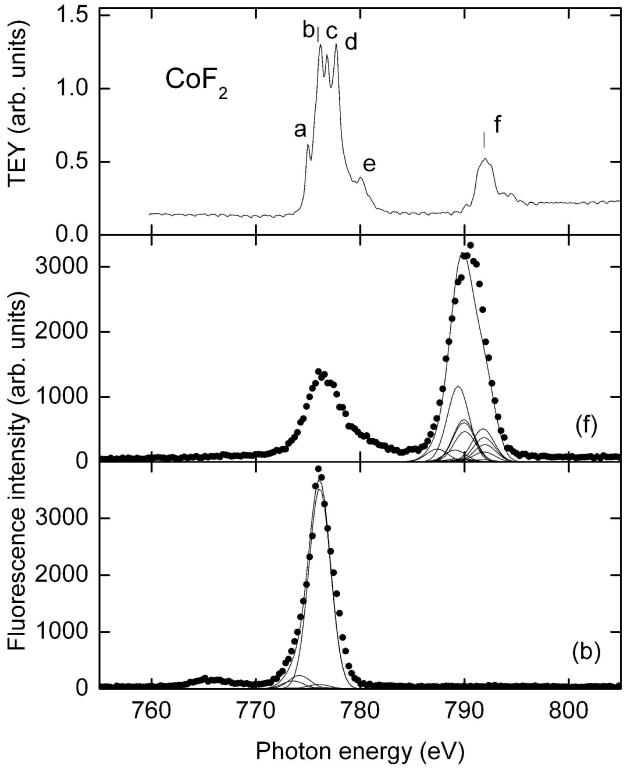

FIGURE 4. Total electron yield (TEY) and resonant emission spectra of CoF_2. Top panel: TEY spectrum. The labels indicate the resonances discussed in the text. Bottom panel: emission spectra obtained when the excitation energy is (b). Middle panel: emission spectra obtained for an excitation energy (f). The solid lines in the emission spectra are the predicted emission lines under the free ion calculation.

this [4,8]. The highest energy peak corresponds to production of quartet terms and the next highest to doublets [4]. Finally, for both compounds there is a broad, weak peak at an even lower emission energy. This emission is due to production of an excited charge transfer state. The main differences between TiO and TiF_2 are the relative intensities of the first three peaks, and the position and width of the charge transfer peak. In MnO the two inelastic peaks are less intense, and the charge transfer peak is broader and closer to the inelastic group. The emission spectra obtained at the second $2p_{1/2}$ absorption peak ((d) in MnO and (e) in MnF_2) are shown in the middle panel of Fig. 3. The high energy structure is almost the same for both, with a weak elastic and two almost equal inelatic peaks. Then there is the normal emission peak that results from decay into a $2p_{3/2}$ hole at the about 639 eV. Between these two groups there are more peaks that correspond to decay into higher states of the ground configuration [4]. In MnO the normal emission peak is more intense and has a charge transfer peak as a low energy shoulder.

Finally, in Fig. 4 we present absorption and emission spectra at the L edge of CoF. As for MnF_2, the TEY spectrum on top of the figure is the one that is compared with the theoretical Co^{2+} spectrum in Fig. 1. This is again the best test case of a Co^{2+} compound. Two emission spectra

are shown in the lower panels, where we make a comparison with the results of the free-ion calculation. The bottom panel shows the spectrum obtained when the excitation energy is at (b). According to the free-ion calculation this is the result of excitation into a single state with $J = 9/2$ that in jj-coupling is the result of the coupling of the $2p_{3/2}$ core hole with a superposition of the $^3F_4$ and $^3F_3$ of the $3d^8$ subshell. Emission has a very sharp elastic peak at 778 eV that shows some asymmetry to the low energy side. This shape is in excellent agreement with the free-ion calculation that predicts strong elastic emission and weak inelastic decay into the $^2G_{9/2}$ and $^2H_{11/2}$ states of the ground configuration. Then the spectrum has a broad, weak peak centered at about 765 eV that is not predicted by the free-ion model. Following the discussion of emission in the titanium and manganese compounds, we think that this emission peak is due to charge transfer. Emission at resonance (f) is shown in the middle panel. The free-ion calculation puts two closely spaced resonances of about the same intensity at this energy. They correspond to production of states with $J = 7/2$ and $J = 9/2$. The experimental emission spectrum is dominated by a broad peak centered at 790.3 eV. This is 1.6 eV below the excitation energy. The free-ion calculation predicts emission into several weak peaks that, when added result in a broad emission peak centered at 789.9 eV. Even though this value is slightly lower than the experimental one, there is good agreement between experiment and theory for the emission shape and width. The experimental emission spectrum also has a weaker normal emission peak at about 776 eV that cannot be predicted by the free-ion calculation. In a separate paper [13] we will present a detailed analysis of these and other emission spectra in the fluorides CoF_2 and NiF_2.

The results presented in this work indicate that x-ray absorption and emission spectroscopies provide very useful information about the electronic structure of transition metal compounds. One can clearly establish differences in the spectra due to different chemical environments. resonant emission spectra also give quantitative information about excited states of the transition metal ground state $3d^n$ configuration. These excited states may be either states resulting from charge transfer or due to spin flip of one or more of the $3d$ electrons. These features are sharper in the fluorides compared to the oxides. The free-ion calculation is also a very good starting point to interpret the experimental results of these soft x-ray spectroscopies.

Acknowledgements

We acknowledge support from DOE-EPSCOR cluster research Grant No. DOE-LEQSF (1993-1995)-03. The Advanced Light Source is funded by the Office of Basic Energy Science, U.S. Department of Energy Contract No. DE-AC03-76SF00098. JJM was supported in part by CONACyT, México, under project No. U41007-F.

1. A. Kotani and S. Shin, Rev. Mod. Phys. **73**, 203 (2001).
2. J. Jia, T. A. Callcott, J. Yurkas, A. W. Ellis, F. J. Himpsel, M. G. Samant, J. Stöhr, D. L. Ederer, J. A. Carlisle, E. A. Hudson, L. J. Terminello, D. K. Shuh, and R. C. C. Perera, Rev. Sci. Instrum. **66**, 1394 (1995).
3. J. Jiménez-Mier, U. Diebold, D. L. Ederer, T. A. Callcott, M. Grush, R. C. Perera, Phys. Rev. B **65**, 184105 (2002).
4. J. Jiménez-Mier, D. L. Ederer and T. Schuler, Phys. Rev. A **72**, # 052502 (2005).
5. R.D. Cowan, *The Theory of Atomic Structure and Spectra* (University of California Press, Berkeley, 1981).
6. F. M. F. de Groot, J. C. Fuggle, B. T. Thole and G. A. Sawatzky, Phys. Rev. B **42**, 5459 (1990).
7. J. Jiménez-Mier, D. L. Ederer and T. Schuler, Phys. Rev. A **68**, # 042715 (2003).
8. S. M. Butorin, J.-H. Guo, M. Magnuson, P. Kuiper, and J. Nordgren, Phys. Rev. B **54**, 4405 (1996).
9. G. van der Laan, Phys. Rev. B **41**, 12366 (1990); G. van der Laan, C.S. Mythen, and H.A. Padmore, Europhys. Lett. **11**, 67 (1990).
10. J. Jiménez-Mier, J. van Ek, D.L. Ederer, T.A. Callcott, J. J. Jia, J. Carlisle, L. Terminello, A. Asfaw, and R.C.C. Perera, Phys. Rev. B **59**, 2649 (1999).
11. B. Gilbert, B. H. Frazer, A. Belz, P. G. Conrad, K. H. Nealson, D. Haskel, J. C. Lang, G. Srajer, and G. De Stasio, J. Phys. Chem. A **107**, 2839 (2003).
12. J. Jiménez-Mier, D. L. Ederer and T. Schuler, Phys. Rev. B **70**, # 035216 (2004).
13. J. Jiménez-Mier, G. Herrera-Pérez and D. L. Ederer, unpublished results.